Analysis of Multi-Quantum Well Electroabsorption Modulators

Joachim Piprek, Yi-Jen Chiu, and John E. Bowers

Electrical Engineering Department, University of California, Santa Barbara, CA 93106

ABSTRACT

Electroabsorption modulators (EAMs) based on the quantum confined Stark effect have advantages in applications that require high speed, low drive voltage, and high extinction ratio. They are promising devices for external signal modulation in high-bandwidth optical communication systems. EAMs can be integrated with other devices like laser diodes, semiconductor optical amplifiers, and mode transformers. We have previously fabricated InGaAsP/InP multi-quantum well EAMs with a bandwidth of 25 GHz and a drive voltage of 1.2 V for 20dB extinction ratio. Further optimization of our devices requires a detailed analysis of internal physical processes and their interaction. In this paper, we employ a two-dimensional electro-optic device model to analyze our EAMs. The model self-consistently combines kp bandstructure and absorption calculations with a carrier drift-diffusion model and optical waveguiding. The required low polarization sensitivity of EAMs leads to strong valence band mixing so that usual effective mass models cannot be applied. Optical transmission characteristics are calculated which are in good agreement with measurements. Modulation efficiency and linearity are analyzed in detail. Optimum operation voltages are identified.

Keywords: quantum confined Stark effect, electroabsorption, quantum well devices, optical modulator, fiber optics, numerical simulation

1. INTRODUCTION

Electroabsorption modulators (EAMs) are attractive for applications requiring high speed modulation, low drive voltage, high extinction ratio and integratibility with lasers. They are promising devices for external signal modulation in high-bandwidth optical communication systems. EAMs can be integrated with other devices like laser diodes, semiconductor optical amplifiers, and mode transformers. EAMs are based on the electroabsorption effect, i.e., on the change of the absorption coefficient due to an electric field. In bulk semiconductors, the absorption edge moves to lower energies with increasing electric field due to a combination of band-to-band absorption and tunneling processes (Franz-Keldysh effect). In quantum wells (QWs), the transition energy between confined energy levels for electrons and holes is reduced as an electric field is applied in growth direction (quantum confined Stark effect, QCSE). This effect is illustrated in Fig. 1. As the field is increased, the overlap of electron and hole wavefunctions is reduced thereby decreasing the absorption strength at the transition energy. Thick quantum wells are advantageous for high field sensitivity (high modulation efficiency) whereas thin quantum wells give stronger absorption. The formation of electron-hole pairs (excitons) in the quantum well enhances the absorption.[1] Compared to bulk materials, quantum well QCSE type modulators have higher modulation efficiencies (lower drive voltage), however, Franz-Keldysh type modulators are less wavelength sensitive (larger optical bandwidth).

We have previously fabricated InGaAsP/InP MQW EAMs with a bandwidth of 25 GHz and a drive voltage of 1.2 V for 20dB extinction ratio.[2] Further optimization of our devices requires a detailed analysis of internal physical processes and their interaction. In this paper, we employ a two-dimensional electro-optic device software[3] to analyze and optimize our EAMs. The model self-consistently combines kp bandstructure and absorption calculations with a drift-diffusion model and optical waveguiding. Section 2 evaluates the quantum well design, Sec. 3 investigates the optical waveguide, and Sec. 4 analyzes optical transmission characteristics.

Email: piprek@ieee.org, Telephone: 1-805-893-4051, Fax: 1-805-893-5440

Physics and Simulation of Optoelectronic Devices X, Peter Blood, Marek Osinski, Yasuhiko Arakawa,
Editors, Proceedings of SPIE Vol. 4646 (2002) © 2002 SPIE · 0277-786X/02/$15.00

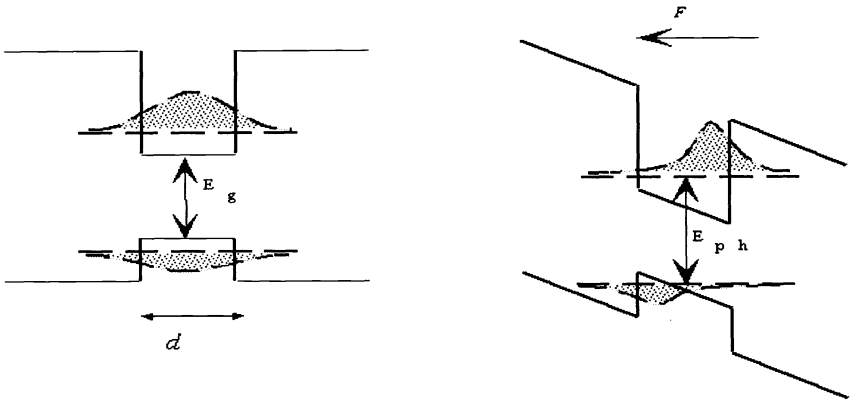

Figure 1. Quantum well band edges, quantum levels, and electron wave functions with (right) and without (left) applied electric field F (E_g - bulk band gap, E_{ph} - transition energy).

2. QUANTUM WELL ACTIVE REGION

Polarization independent performance is an important requirement in many applications of electroabsorption modulators. In the InGaAsP/InP material system, TE polarized waves mainly generate heavy holes whereas TM polarized waves only generate light holes during the absorption process. The corresponding dipole matrix elements result in the absorption coefficients

$$\alpha_{TE} = \frac{1}{4}\alpha_{LH} + \frac{3}{4}\alpha_{HH} \quad (1)$$

$$\alpha_{TM} = \alpha_{LH} \quad (2)$$

where α_{HH} and α_{LH} are the absorption coefficients for heavy and light holes, respectively. Thus, $\alpha_{HH} = \alpha_{LH}$ is a basic requirement for polarization insensitive modulation. In unstrained quantum wells, the transition energy for heavy holes is lower than for light holes due to the different effective mass. To align the absorption edges, the light hole bandgap needs to be reduced by using tensile strain in the quantum well. The barrier layers are compressivelly strained for strain compensation. For those reasons, the active region of our example device is comprised of ten $In_{0.485}Ga_{0.515}As_{0.979}P_{0.021}$ quantum wells that are 10.4 nm thick and that exhibit 0.37% tensile strain. The $In_{0.923}Ga_{0.077}As_{0.325}P_{0.675}$ barriers are 7.6 nm thick with 0.5% compressive strain. Calculated absorption spectra are plotted in Fig. 2. The absorption edges are almost identical for TE and TM polarized waves.

The degeneration of heavy and light hole levels in our quantum wells is accompanied by an enhanced interaction of both particles. This interaction causes a substantial deformation of the valence subbands (valence band mixing). Fig. 3 shows the resulting non-parabolic shape of the valence bands, i.e., the effective mass model of parabolic bands cannot be applied here. The fundamental absorption edges in Fig. 2 are dominated by the first subbands (HH1, LH1), higher subbands cause additional steps in the absorption spectrum.

Both the absorption spectrum and the refractive index spectrum change with the QW carrier density. The ratio of both these changes give the chirp factor α_H (linewidth enhancement factor). A slightly negative chirp factor is ideal for long fiber optic transmission distances.[4] It is typically between 4 and 6 for semiconductor

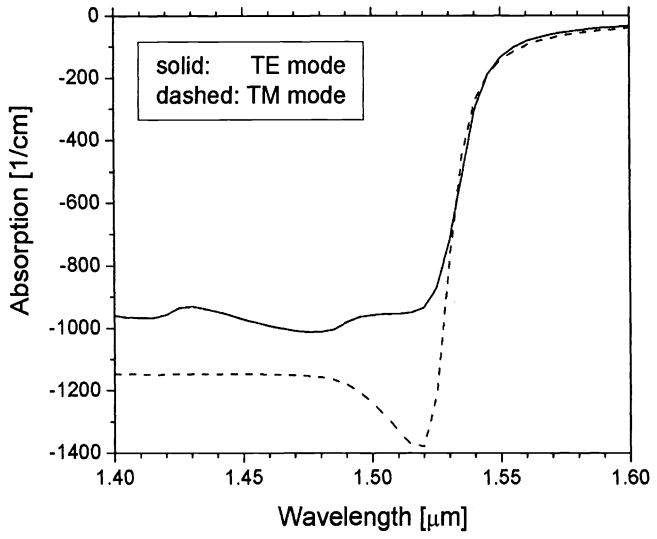

Figure 2. Quantum well absorption spectra for TE and TM polarization, respectively, at zero bias.

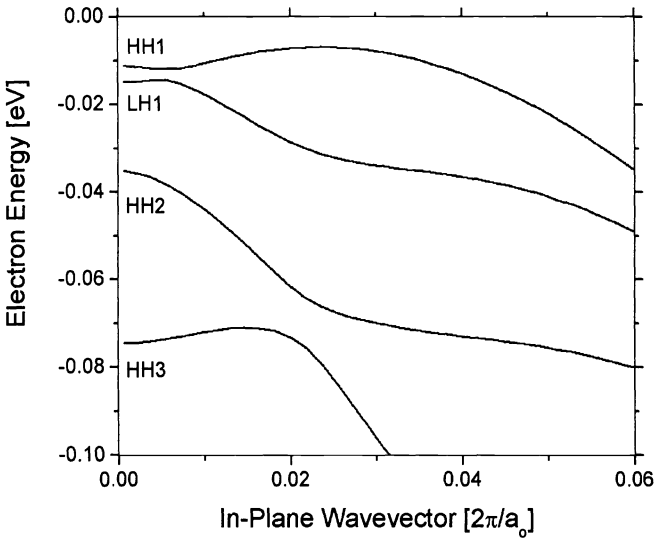

Figure 3. Valence subbands for polarization insensitive design (HH# - heavy hole subbands, LH# - light hole subbands).

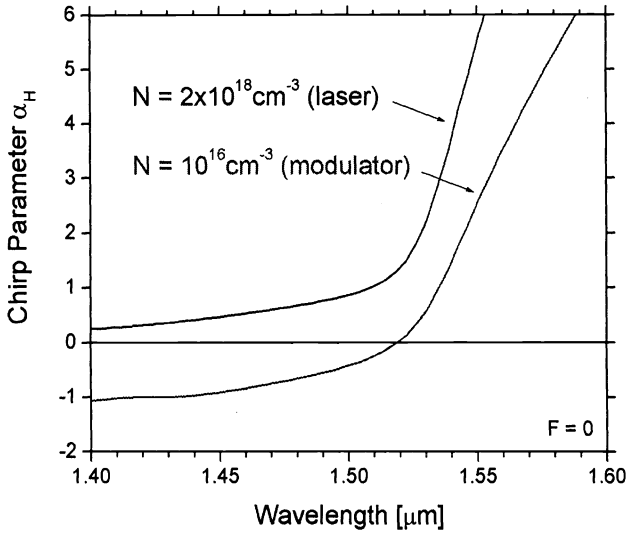

Figure 4. Chirp parameter as function of photon wavelength for low (modulator) and high (laser) carrier densities.

lasers, while it is close to zero or even negative for electroabsorption modulators. Figure 4 compares both cases for our quantum well. High carrier densities are typical for laser diodes and do not allow for negative chirp factors. Modulators are reverse biased and exhibit a much lower carrier density in the quantum wells. In Fig. 4, the transition wavelength to negative chirp factors is about 1.52μm which is near the absorption peak (cf. Fig. 2). Since the modulator rather operates in the tail region of the absorption spectrum, the chirp factor is expected to be near $\alpha_H = 2$ in our case.

The energy band diagram of our multi-quantum well (MQW) active region is plotted in Fig. 5 at zero bias, indicating a significant build-in electrostatic field. Including the undoped InP regions, the total intrinsic (i) region thickness of our *pin* structure is about 300 nm. Figure 6 shows the internal field for different applied voltages. At 1V forward bias, the MQW field vanishes and the band edges are flat. At typical reverse bias values of -1V to -2V, the internal field is close to 100 kV/cm. At this high field strength, excitons are assumed to be eliminated in our device.

3. OPTICAL WAVEGUIDE

Our example device utilizes a ridge structure for waveguiding with a 2μm wide ridge etched beyond the intrinsic region. The fundamental optical mode is shown in Fig. 7 for half the device cross section. The narrow ridge eliminates higher order modes and it gives a more circular mode profile for better coupling to optical fibers. The vertical refractive index profile is plotted in Fig. 8 together with the mode intensity. The optical confinement factor is $\Gamma = 0.2$. Stronger optical confinement is desired for low voltage operation, however, it causes higher fiber coupling losses. The optical model includes absorption losses by intraband transitions of free carriers and by intervalence band transitions. Both are roughly proportional to the carrier density and only relevant in p-doped regions ($\alpha_p \approx k_p p$ with $k_p = 25 \times 10^{-18}\text{cm}^2$). Figure 8 shows the resulting absorption profile. Due to the small overlap with the optical mode, the modal optical loss due to holes is only 1.5 cm^{-1}. Stronger optical losses are usually caused by photon scattering at the rough sidewalls of the etched waveguide, however, scattering losses are hard to calculate. The strongest contribution to the internal optical loss seems to result from the residual interband absorption at zero voltage which can be estimated as 29 cm^{-1} (Fig. 2).

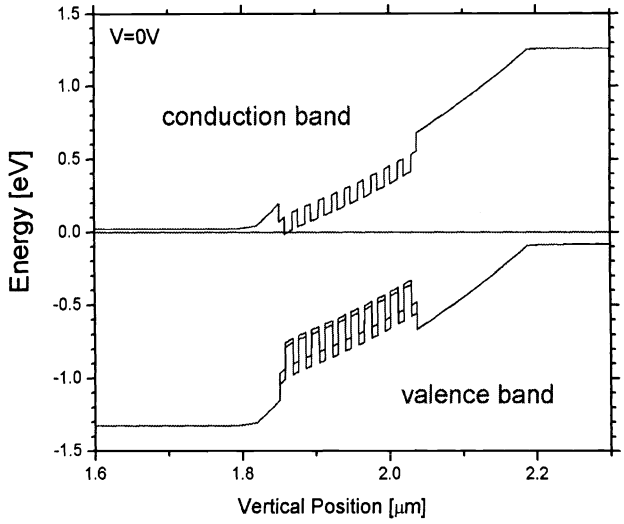

Figure 5. Energy band diagram of MQW active region with edges of heavy hole band, light hole band, and conduction band.

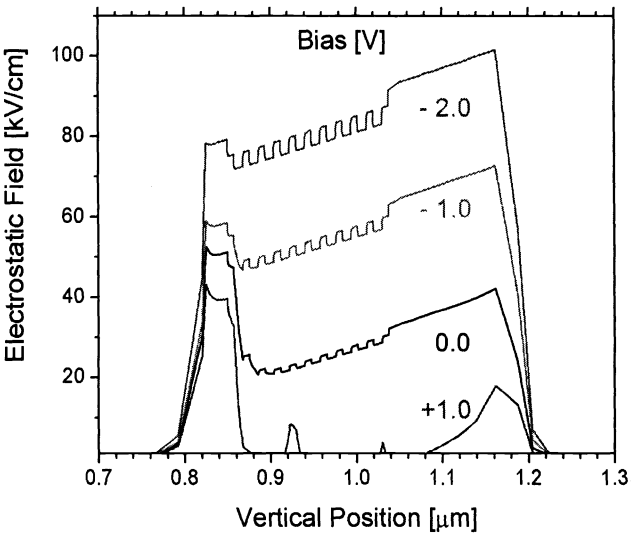

Figure 6. Internal electrostatic field at different applied voltages.

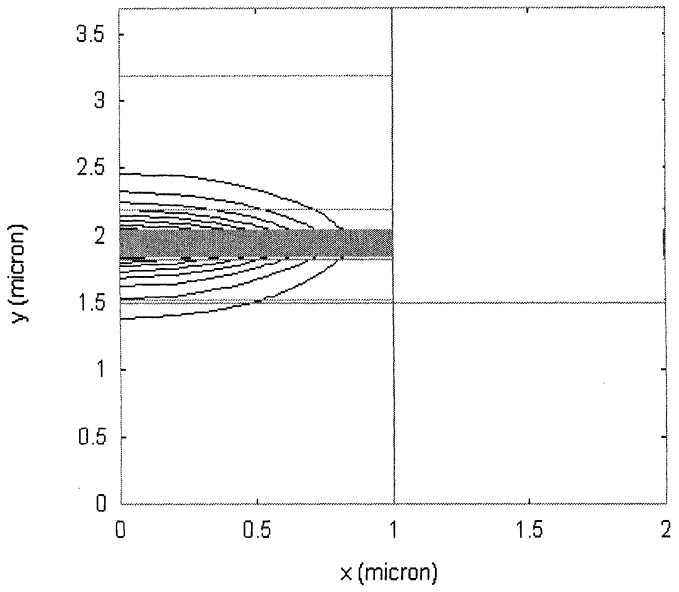

Figure 7. Half cross-section of the modulator waveguide with fundamental optical mode (the left border is the vertical symmetry plane of the device, the narrow lines indicate the MQW).

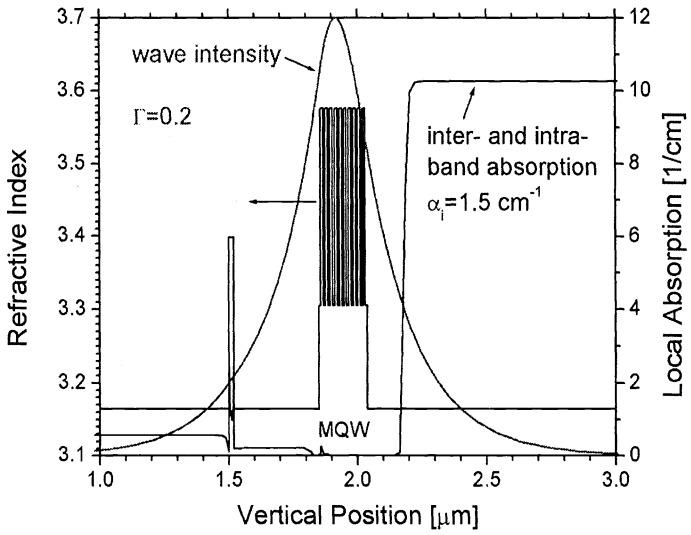

Figure 8. Vertical profile of refractive index, optical mode, and hole related absorption.

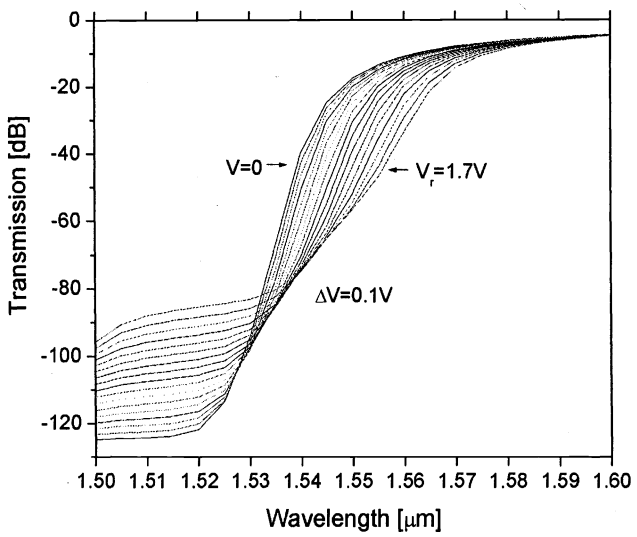

Figure 9. Optical transmission vs. wavelength with the reverse bias as parameter.

4. TRANSMISSION ANALYSIS

The optical transmission $T(\lambda, V)$ of the modulator is a function of the wavelength λ and of the applied reverse voltage V

$$T(\lambda, V) = \gamma^2(1-R)^2 \exp -\Gamma\alpha_{QW}(\lambda, V)L. \tag{3}$$

(device length $L = 300$ μm). The fiber coupling coefficient γ gives the overlap of the optical modes of fiber and modulator. The facet reflectance R is kept low by antireflection coating. In our case, the optical loss at each facet is $\gamma(1-R)$ = -3dB. The calculated transmission characteristics are shown in Fig. 9 as function of wavelength with the bias as parameter. As expected, with increasing reverse bias, the absorption edge moves towards longer wavelengths and the maximum absorption is reduced. Let us evaluate the transmission at 1550 nm wavelength. At zero bias, the residual transmission of -17dB is excellent agreement with the measured result,[2] confirming our loss analysis above. A bias of -1.2V gives -44dB transmission, which is only slightly lower than measured. The difference gives an extinction ratio of 27dB. In accordance to typical measurements, Fig. 10 displays the same transmission T as function of voltage with the wavelength as parameter. Minimum absorption occurs at the upper end of the spectrum (1600 nm) and maximum absorption at the lower end (1500 nm). At 1550nm, the transmission is reduced with higher reverse voltage, as discussed for Fig. 9.

The steepest slope of $T(V)$ occurs at about 1V reverse voltage, which gives the highest modulation efficiency. However, practical applications also require high total light transmission. Therefore, we here use $T \times dT/dV$ as figure of merit which is plotted in Fig. 11 for three different wavelengths. The optimum voltage for maximum efficiency is slightly below 1V for 1550 nm wavelength. Fig. 11 emphazises the strong wavelength dependence of quantum-well EAM performance which was already indicated by the previous two figures.

Linearity is another main requirement in practical applications of EAMs. Ideally, both the second derivative d^2T/dV^2 and the third derivative d^3T/dV^3 of the transmission function $T(V)$ should be zero. However, this is hard to achieve and we are using the sum of both the derivatives as figure of merit which is plotted in Fig. 12. At 1550 nm wavelength, the optimum reverse bias for maximum linearity is close to 0.7 V since both the derivatives compensate each other at this voltage. The figure of merit shows a maximum at the voltage of highest efficiency (0.95 V). Thus, maximum efficiency and maximum linearity cannot be achieved simultaneously. The optimum voltage of our EAM depends on the specific application.

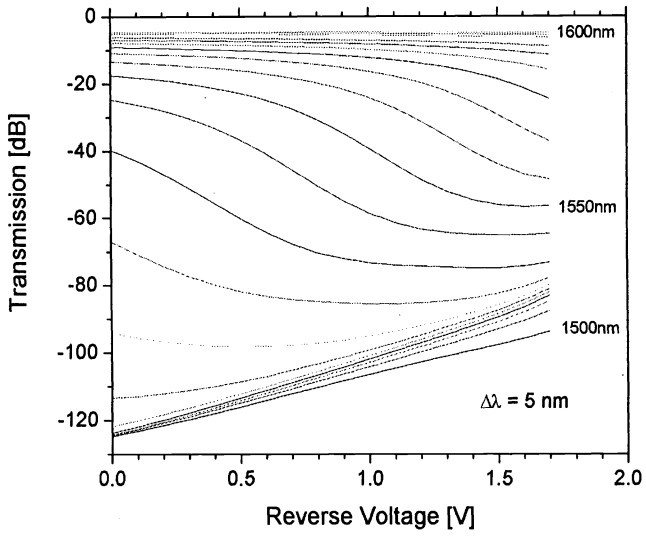

Figure 10. Optical transmission vs. reverse bias with the wavelength as parameter.

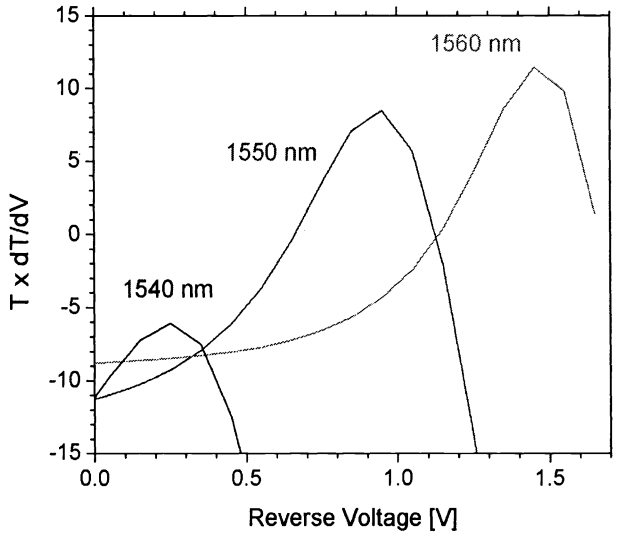

Figure 11. Transmission T [dB] times dT/dV [dB/V] as function of reverse bias for three different wavelengths.

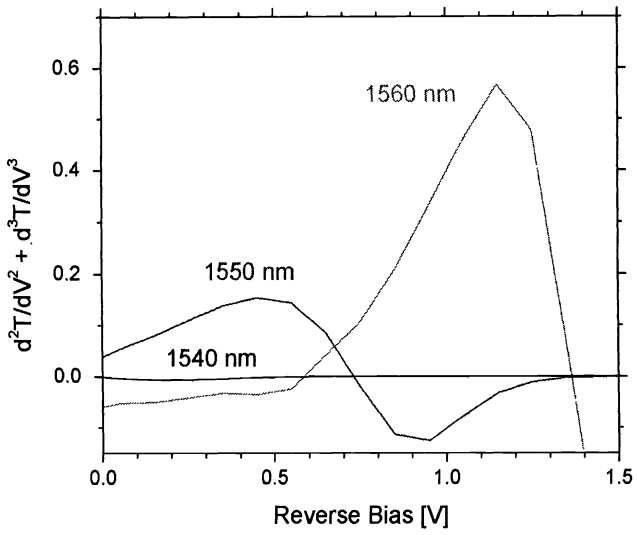

Figure 12. Sum of second and third derivative of the transmission function T(V) as function of reverse bias for three different wavelengths.

5. SUMMARY

Based on two-dimensional simulation of carrier transport, optical absorption, and optical waveguiding, we have analyzed internal physics of multi-quantum well electroabsorption modulators. Polarization insensitivity of the quantum confined Stark effect is obtained by using tensile strain in the quantum wells. This causes strong valence band mixing so that common effective mass theories are invalid in our case. Strong internal electrostatic fields close to 100 kV/cm are calculated for typical reverse bias operation. The internal optical loss is found to be dominated by residual quantum well absorption. The calculated transmission characteristics exhibit a strong wavelength sensitivity. For transmission at 1550 nm, optimum reverse voltages are identified for maximum efficiency and maximum linearity, respectively.

REFERENCES

1. D. A. B. Miller, D. S. Chemla, T. C. Damen, A. C. Gossard, W. Wiegmann, T. H. Wood, and C. A. Burrus, "Electric field dependence of optical absorption near the band gap of quantum well structures," *Physical Review B* **32**, pp. 1043–1059, 1985.
2. S. Z. Zhang, Y.-J. Chiu, P. Abraham, and J. E. Bowers, "25-GHz polarization-insensitive electroabsorption modulators with traveling-wave electrodes," *IEEE Photonics Technology Letters* **11**, pp. 191–193, 1999.
3. LASTIP 6.1.1 by Crosslight Software, 2001.
4. G. Agrawal, *Fiber-Optic Communication Systems*, Wiley, Singapore, 1993.